

# Using Redundant and Disjoint Time-Variant Soft Robotic Sensors for Accurate Static State Estimation

Thomas George Thuruthel , Josie Hughes , *Member, IEEE*, Antonia Georgopoulou , Frank Clemens ,  
and Fumiya Iida , *Senior Member, IEEE*

**Abstract**—Soft robotic sensors have been limited in their applications due to their highly nonlinear time variant behavior. Current studies are either looking into techniques to improve the mechano-electrical properties of these sensors or into modelling algorithms that account for the history of each sensor. Here, we present a method for combining multi-material soft strain sensors to obtain equivalent higher quality sensors; better than each of the individual strain sensors. The core idea behind this work is to use a combination of redundant and disjoint strain sensors to compensate for the time-variant hidden states of a soft-bodied system, to finally obtain the true strain state in a static manner using a learning-based approach. We provide methods to develop these variable sensors and metrics to estimate their dissimilarity and efficacy of each sensor combinations, which can double down as a benchmarking tool for soft robotic sensors. The proposed approach is experimentally validated on a pneumatic actuator with embedded soft strain sensors. Our results show that static data from a combination of nonlinear time variant strain sensors is sufficient to accurately estimate the strain state of a system.

**Index Terms**—Soft sensors and actuators, sensor fusion, modeling, control, learning for soft robots.

## I. INTRODUCTION

SOFT robotic sensors have immense potential to revolutionize the field of health-monitoring, human motion detection, human-machine interfaces, and soft robotics, owing to their high conformability [1]. Yet, the applications of these sensors have been limited primarily because of the challenges in modelling these sensors [2]. Irrespective of their stimuli responsive mechanism, all of these sensors suffer from a combination of nonlinearity, hysteresis, drift, overshoot and slow response [1].

Manuscript received October 23, 2020; accepted February 16, 2021. Date of publication February 23, 2021; date of current version March 10, 2021. This letter was recommended for publication by Associate Editor G. Krishnan and Editor Kyu-Jin Cho upon evaluation of the reviewers' comments. This work was supported by the SHERO project, a Future and Emerging Technologies (FET) programme of the European Commission under Grant ID 828818. (*Corresponding author: Thomas George Thuruthel.*)

Thomas George Thuruthel, Josie Hughes, and Fumiya Iida are with the Bio-Inspired Robotics Lab, Department of Engineering, University of Cambridge, Cambridge CB2 1PZ, U.K. (e-mail: tg444@cam.ac.uk; jaeh2@cam.ac.uk; fi224@cam.ac.uk).

Antonia Georgopoulou is with the Department of Functional Materials, Empa – Swiss Federal Laboratories for Materials Science and Technology, Dübendorf 8600, Switzerland, and also with the Vrije Universiteit Brussel (VUB), and Flanders Make Pleinlaan 2, Brussels B-1050, Belgium (e-mail: antonia.georgopoulou@empa.ch).

Frank Clemens is with the Department of Functional Materials, Empa – Swiss Federal Laboratories for Materials Science and Technology, Dübendorf 8600, Switzerland (e-mail: frank.clemens@empa.ch).

Digital Object Identifier 10.1109/LRA.2021.3061399

This can be attributed to the complex visco-elastic properties of the sensor and its surrounding material.

The literature on the different types of soft sensors is wide and immense. Here, we focus mainly on soft strain sensors, as they are the most widely used. Their functional materials vary from liquid conductors [3]–[5], nanocomposites [6]–[8], optical [9] and so forth. Several studies incorporate additional functionalities such as self-healing [10], [11], 3D printing [12], etc. However, all of these sensors suffer from highly nonlinear effect, either by itself or when they are embedded inside a soft matrix [1], [2]. Depending on the strain responsive mechanism, this can be because of the rearrangement of conductive particles [13], damage, geometric effects induced by the surrounding visco-elastic matrix and/or de-lamination due to impedance mismatch [14]. Solving these problems from the material side is still an open challenge which is also hampered by the unavailability of benchmarking tools for comparing different technologies.

Recent advancements in machine learning can be an alternate solution to handling the nonlinear time-variant dynamics of these soft sensors [15], [16]. This can be done by explicitly providing the past sensor information [17], by using recurrent neural networks that can retain information about the past data [18]–[20], or by using adaptive algorithms [21]. Both approaches, however, have common disadvantages. By converting the static state estimation problem into a dynamic one, the modelling approach has to be now discretized and sampled at a fixed rate. Coupled with the computational overhead of recurrent neural networks, this also increases the hardware requirements for sensor modelling. It is also more difficult to generate samples for and train recurrent networks [22]. Moreover, due to the models past dependence on the sensor data, initialization of the network becomes complicated.

This work presents a novel alternate method to estimate the true strain state of a soft bodied system using redundant and disjoint strain sensors. The core idea is to use the additional conditional mutual information obtained from multiple strain sensors, strained by the same amount, to compensate for the hidden states of visco-elastic body. We provide a method for obtaining disjoint sensors by using multi-material sensory matrix, similar to a work done for enhancing the gauge factor of strain sensors [23]. The information theory concept of mutual information is introduced as a numerical method to estimate the quality of these nonlinear soft strain sensors and their combination, which is verified using machine learning tools. The proposed approach is verified experimentally using custom

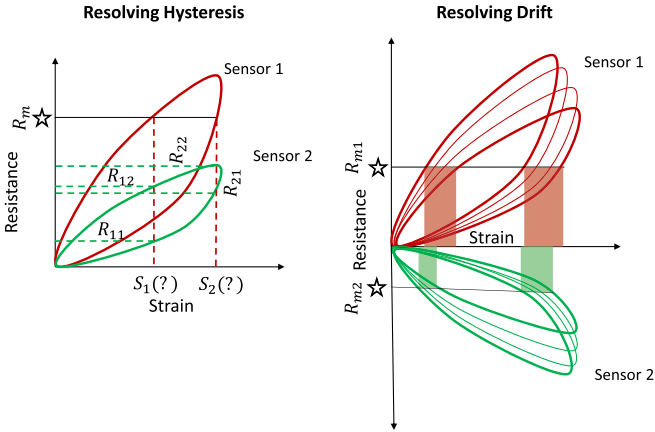


Fig. 1. A visualization of resolving uncertainties in the true strain state using redundant and disjoint sensors. At least two dissimilar sensors are required for hysteresis resolution (Left). Uncertainties in the strain state can be reduced with redundant sensors in the case of the drift (Right).

made testing devices and on a simple pneumatic actuator. The main contribution of this work is to show that redundant and variable soft strain sensors can be combined in a static manner to compensate for time variant non-linearities in soft strain sensors. In addition, we present simple statistical techniques that can be used for quantifying the quality of a soft strain sensor and its combinations with any complex modelling techniques.

## II. THEORY

The time varying behavior of a soft strain sensor is due to several unobservable physical factors that may or may not be dependent on the straining history. Hysteresis, for example, occurs due to internal friction in the material, which is typically modelled as a strain-rate dependent phenomenon. This makes the response of a soft strain sensor to be a function of the current strain and the other hidden states (for instance, stress, strain rate, etc). As most of these hidden states are a function of the straining history, this can also be estimated using the past data of strain. Alternatively, these hidden states can also be estimated using multiple sensors that undergo the same straining history, but have varying dependencies on the hidden states. A visualization of resolving uncertainties in the true strain state using redundant sensors is shown in Fig. 1, for two typical time-varying behaviors. Here, for the simplified hysteresis model, we assume that resistance of the sensor is a function of the true strain and the sign of the strain rate. Hence, the strain rate direction will be the hidden state that cannot be observed using a single strain sensor. Every observed resistance ( $R_m$ ) can correspond to two possible strain states ( $S_1$  or  $S_2$ ) caused by the binary ambiguity on possible strain rate direction (Shown by the two unknown states in Fig. 1). By addition of an additional distinct strain sensor, the true state can be resolved. This is because the two possible strain states create four unique resistance states. Strain  $S_1$  can only cause resistance  $R_{11}$  or  $R_{12}$ , while Strain  $S_2$  can only cause resistance  $R_{21}$  or  $R_{22}$ . In other words, using another sensor, the hidden strain rate direction can be estimated.

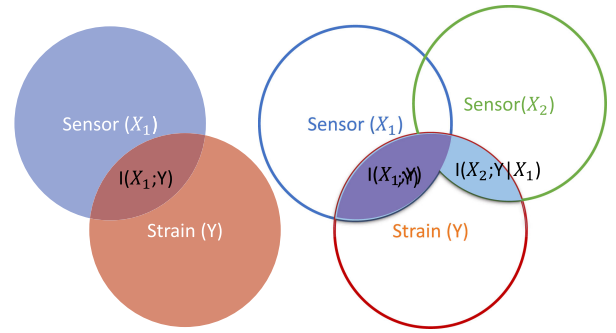


Fig. 2. The mutual information ( $I(X_1; Y)$ ) of two random variables provides the amount of information obtained about one random variable through observing the other random variable. The same measure can be extended to multiple variables with the conditional mutual information  $I(X_2; Y | X_1)$ .

For more complex hysteresis models, more sensors would be required for full resolution, based on the number of hidden states. Drift, on the other hand, cannot be fully resolved with multiple sensors, but the uncertainty on the true strain values can be reduced with the addition of more and more sensors. For every measured sensor resistance, the possible strain state can be narrowed down to two bands of strain regions. Looking at the intersection of these bands among all the sensors help in reducing the uncertainty further. Other time variant non-linearities can be resolved similarly. Note that redundant sensors can be still be useful even if the sensors are exactly the same to reduce noise and improve resolution of the sensor.

Given that temporal non-linearities can be resolved to varying extends with dissimilar sensor networks undergoing the same strain, we now go to the problem of quantitatively comparing two sensors. Here, we propose the information theory metric of mutual information as an empirical measure of the *quality* of a sensor [24]. As modelling of these kind of sensors are near impossible, we have to resort to empirical ways to test and evaluate each sensor. In information theory, the mutual information (MI) of two random variables is a measure of the mutual dependence between the two variables. MI is a more general notion in information theory that quantifies the expected amount of information held in a random variable. The mutual information  $I(X; Y)$  between two random variables  $X$  and  $Y$  is the amount of information  $X$  gives about  $Y$  (Fig. 2). Mathematically, we define this as the difference between the entropy of  $X$  ( $H(X)$ ) and the entropy of  $X$  conditioned on knowing  $Y$  ( $H(X|Y)$ ).

$$I(X; Y) = H(X) - H(X|Y) \quad (1)$$

$X$  is a random variable with distribution  $P_X = (P_1, \dots, P_k)$  over a finite set of possible outcomes  $\Omega = \{1, \dots, k\}$  and,

$$H(X) = \sum_{x \in \Omega} P_x \log \frac{1}{P_x} \quad (2)$$

The conditional entropy of  $X$  conditioned on another random variable  $Y$  with distribution  $P_Y$  is:

$$H(X|Y) = -\mathbb{E}_{P_Y}[H(X|Y = y)] \quad (3)$$

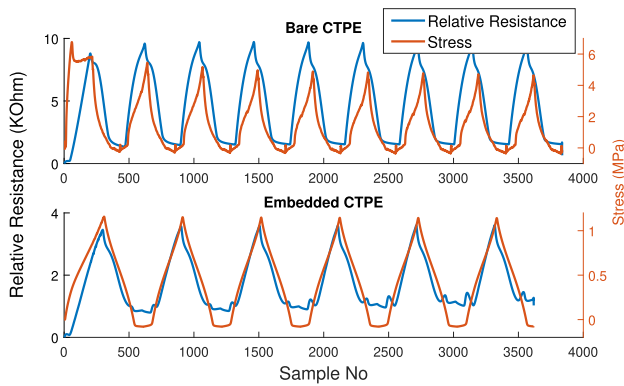


Fig. 3. Response of the CTPE sensor to a cyclic triangular strain wave profile. The strain profile is not shown for clarity.

Mutual information is symmetric, i.e.  $I(X; Y) = I(Y; X)$ . The higher the mutual information between the strain and sensor data, the better the sensor performance as a static strain sensor. Along the same lines, if the MI of sensor  $X_2$  is higher than sensor  $X_1$  ( $I(X_2; Y) > I(X_1; Y)$ ), then it can be concluded that sensor  $X_2$  will perform better than sensor  $X_1$ .

Correspondingly, the performance of multiple sensors can be quantified by their combined mutual information (Fig. 2). Finally, dissimilarity between two sensors can be quantified by their conditional mutual information ( $I(X_1; Y|X_2)$ ). The combined mutual information is written as:

$$I(X_1, X_2; Y) = I(X_1; Y) + I(X_2; Y|X_1) \quad (4)$$

The conditional mutual information can be obtained from the joint entropies by the chain rule:

$$I(X_2; Y|X_1) = H(X_2, X_1) + H(Y, X_1) - H(X_2, Y, X_1) - H(X_1) \quad (5)$$

Note that to obtain all the described measures, it is necessary to uniformly sample for all possible strain within its range.

### III. MATERIAL CHARACTERIZATION

This section presents the soft strain sensor that we are using for our tests, its characterization and the process for obtaining different behaviors from these sensors.

#### A. Conductive Thermoplastic Elastomer (CTPE)

The sensor we are using for our tests is a composite made from a mixture of a thermoplastic elastomer and carbon black extruded in the form of a cylindrical wire [6]. Upon stretching the conductive particles rearrange and the geometry of the sensor changes, causing a change in the base resistance of the sensor. The response of the CTPE sensor when it is bare and when it is surrounded by an embedding matrix (Ecoflex-20) to a triangular strain wave profile is shown in Fig. 3. The straining is done till 140% for both cases, with cycle times of 22 and 30 seconds respectively. It is observable that the response of the CTPE sensor is not just dependent on the strain profile, but also on the current stress values. This can be validated by using

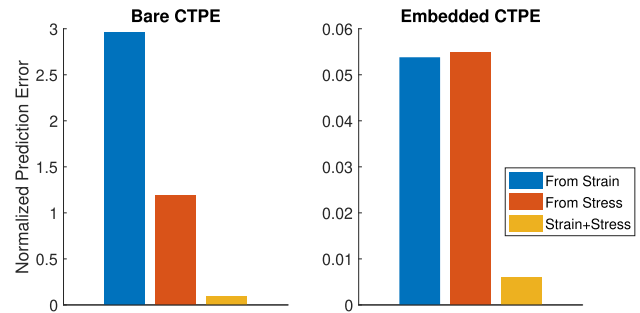


Fig. 4. Physical factors and their effect on the electrical response of the CTPE sensor. It can be seen that the electrical response of the sensor is highly dependent on the current stress and strain.

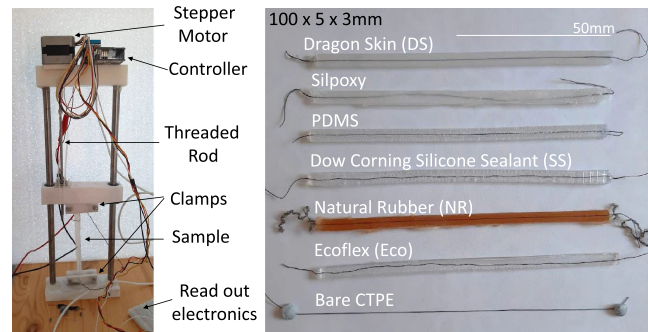


Fig. 5. Experimental setup for studying change in sensor behavior with surrounding matrix.

a simple feedforward neural network to predict the resistance values using the strain and stress values as input. Here, we are using an artificial neural network to measure the dependency between a multivariate nonlinear mapping. The results of the prediction analysis is shown in Fig. 4. It is evident that both the current stress and strain values affect the electrical response of the CTPE sensor, irrespective of the surrounding medium. The internal stress value is one of the hidden states that has to be estimated/compensated for obtaining the true strain values. Note that the stress values can be estimated using the straining history, but as mentioned previously, such modelling approaches are highly undesirable. As stress distribution is a significant factor to the response of the CTPE sensor, we can obtain varying behaviors from the CTPE sensor by simply changing the surrounding matrix of the sensor which is validated in the next section.

#### B. Multi-Material Sensor Matrix

In order to investigate materials we can use for varying the behavior of the CTPE sensor, we develop a test setup as shown in Fig. 5. Six commonly used elastomeric matrices are used to cover the CTPE sensor and their corresponding strain/resistance behavior is investigated. Two samples of each material are made to ensure that the behavioral change is repeatable. The materials we used are Dragon Skin-20 (©Smooth-On, Inc), Ecoflex-20 (©Smooth-On, Inc), SYLGARD 184 Silicone Elastomer (©The

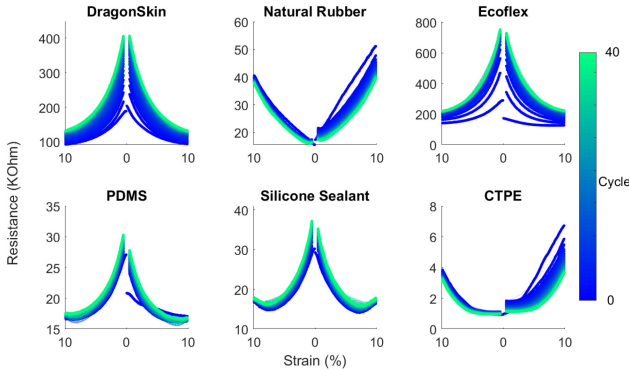


Fig. 6. Cyclic straining tests for each sample of CTPE surrounded with different matrix. Two samples of each material is tested for ensuring repeatability (shown in the mirrored X Axis). Only values in positive straining is shown for interpretability.

Dow Chemical Company), Dow Corning Silicone Sealant, Sil-Poxy Silicone Adhesive (©Smooth-On, Inc) and Natural Rubber (©East Coast Fibreglass Supplies).

Cyclic tests are performed on each sample (Fig. 6). The Sil-Poxy Silicone Adhesive was the only material that showed drastically unrepeatable performance and was hence removed from our further studies. All the other samples showed high repeatability in their nonlinear behavior among samples, even though their properties changed significantly from the bare CTPE sensor. This means that although the matrix affects the nonlinear behavior of the sensor, this effect is consistent and repeatable for a specific matrix. For example, the platinum cured silicone elastomers DragonSkin and Ecoflex had an order of magnitude change in their base resistance while curing and had much higher drift, but this shift in base resistance and the drift characteristics are repeatable among the two samples. Knowing that varying, but repeatable properties can be obtained by changing the surrounding matrix of the soft strain sensor, we next investigate how such sensors can be combined to get superior performance.

#### IV. RESULTS

##### A. Static Strain Estimation

To investigate how these developed sensor samples can be combined for static strain estimation we perform further tests using the experimental setup shown in Fig. 5. Seven embedded sensor samples are randomly selected and mounted on the linear straining device. Pseudo-random straining of the samples are performed in parallel and their corresponding resistance's are measured. This is to ensure that straining occurs at varying frequencies and amplitudes to induce all the nonlinear configurations. The motion is limited to the maximum strain of 40 % to avoid damages and plastic deformation of the sensor. This causes each samples to have the same strain profile but varying effects on their hidden states. The ability of a simple feedforward neural network to estimate the true strain values from different combinations of strain sensors is investigated along with the

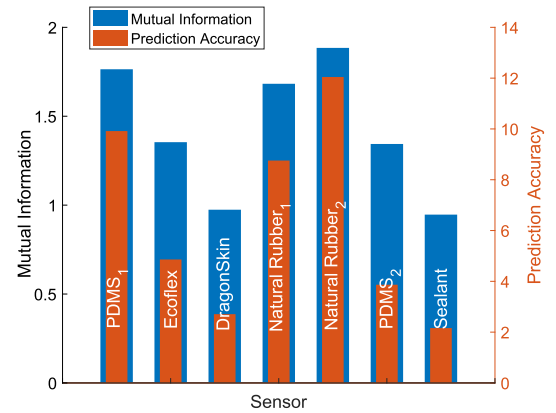


Fig. 7. Strain prediction accuracy and Mutual Information of each embedded soft sensor.

validation of Mutual Information as an indicator of the sensor performance.

A sample size of 8000 data points is obtained for training the neural network and estimation the mutual information values. A single layer neural network with tanh activation functions and a hidden layer size of 60 is used for learning the mapping from the sensor resistances to the strain values. Levenberg-Marquardt backpropagation is used for training the network with a training, testing and validation set divided in the ratio 70:15:15 respectively. The validation set ensures that overfitting is unlikely. The training is performed in the MATLAB environment. For calculating the Mutual information of each sensor and their combinations, a public toolbox, MIToolbox is used [25]. Note that as the MI of random variables depend on the resolution of the measuring device, the discrete values obtained directly from the data acquisition system is used (12 bits).

The prediction accuracy for each individual sensor along with their mutual information (1) with the strain values is shown in Fig. 7. The prediction accuracy is measured as the inverse of the mean squared error of the estimated strain for all the sample. As expected, natural rubber which showed low drift and higher linearity to strain performs the best, but only by a small margin. As the behavior of these sensors are highly nonlinear, it is difficult to predict their performance based on visual inspection. Testing by training on a neural network is one solution, but it is time consuming and dependent on the architecture of the network. Mutual Information, on the other hand, is a quick and powerful metric to estimate the *quality* of a sensor (Fig. 7). For instance, measuring the MI of a single sensor took on average 24  $\mu s$ , while measuring the combined MI of two sensor took on average 840  $\mu s$ . Note that the accuracy results shown here are specific to the input (i.e linear strain) and not necessarily transferable to other sensing objectives like shear, pressure, etc.

Extending the same methodology (4) to two sensors combinations (21 in total), we can obtain similar results as we observed for the single sensor case, with small deviations due to noise (Fig. 8). The mutual information measure is a robust indicator of the best and worst combinations of the embedded soft sensors for

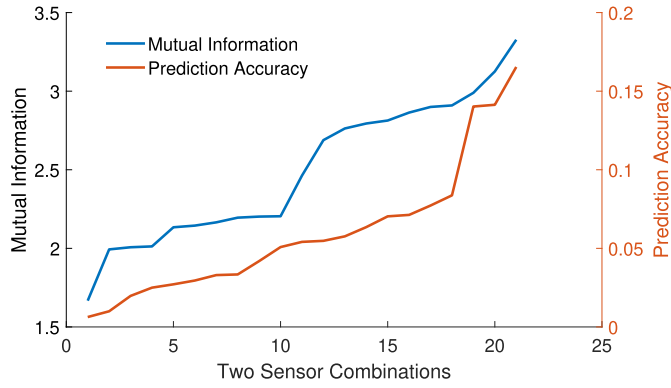


Fig. 8. Strain prediction accuracy and Mutual Information for all 21 combinations of double sensors. The sensor combinations are sorted by their mutual information for comparison.

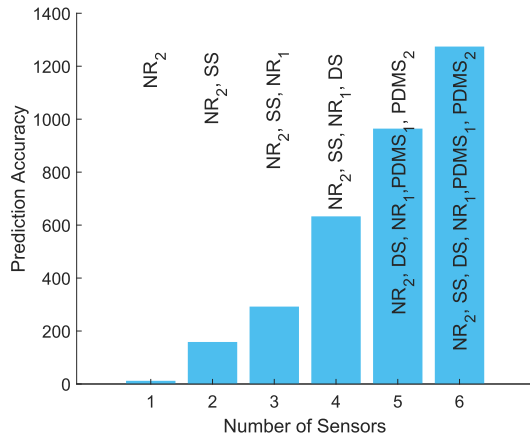


Fig. 9. Improvement in static strain sensing accuracy with the addition of redundant and disjoint soft strain sensors. The prediction accuracy for the best combination is shown here.

strain measurement. Note that the MI metric is obtained through statistical techniques without any modelling involved, which is highly desirable for soft strain sensors.

The best prediction accuracies for all number of redundant sensor configurations are shown in Fig. 9. As expected, with higher number of sensors, the prediction accuracy also becomes higher. Interestingly, the performance of the combined sensor systems is independent from the individual sensor performances. For instance, the silicone sealant is the worst performing sensor matrix by itself, however, in combination with one of the Natural Rubber embedded sensor, we get the best performing combination for a two sensor configuration. Such observations can only be obtained through statistical techniques we show here or with learning based approaches. Traditional tools like measuring linearity, hysteresis, drift, etc can be used for evaluating a single soft sensor, but is not extendable to sensor combinations. It must be pointed out that in our analysis we have kept the sensors separate from each other, which is not a realistic scenario. In the next section we show how the multi-material embedded sensors can be used for practical purposes.

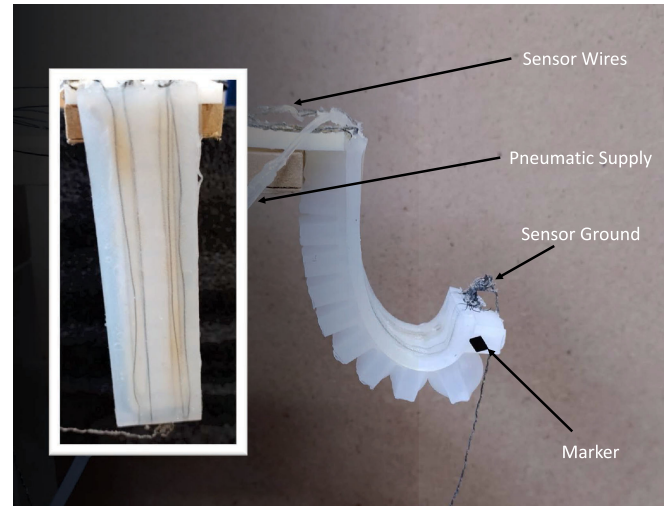


Fig. 10. Experimental Setup for predicting bending state from the static sensor data.

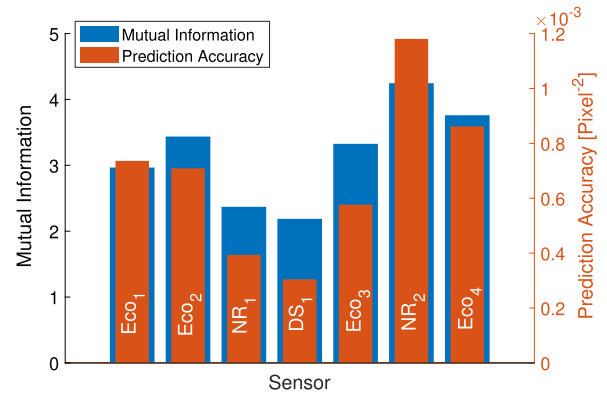


Fig. 11. Strain prediction accuracy and Mutual Information of each embedded soft sensor for the bending actuator.

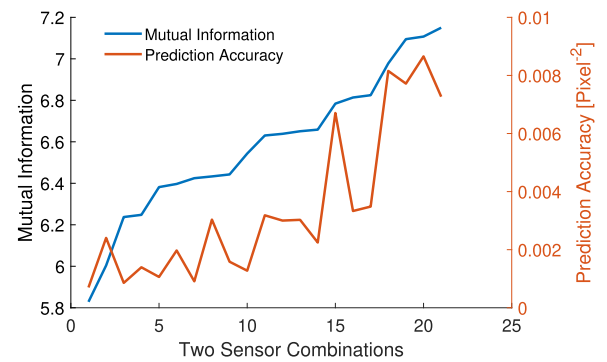


Fig. 12. Strain prediction accuracy and Mutual Information for each combination of two embedded soft sensor for the bending actuator. The sensor combinations are sorted by their mutual information for comparison.

**B. Case Study: Pneumatic Actuator**

In order to validate the applicability of our proposed method for practical applications, we develop a one Degree of Freedom soft pneumatic bending actuator with seven embedded sensors (Fig. 10). As all the sensors have to be finally embedded in

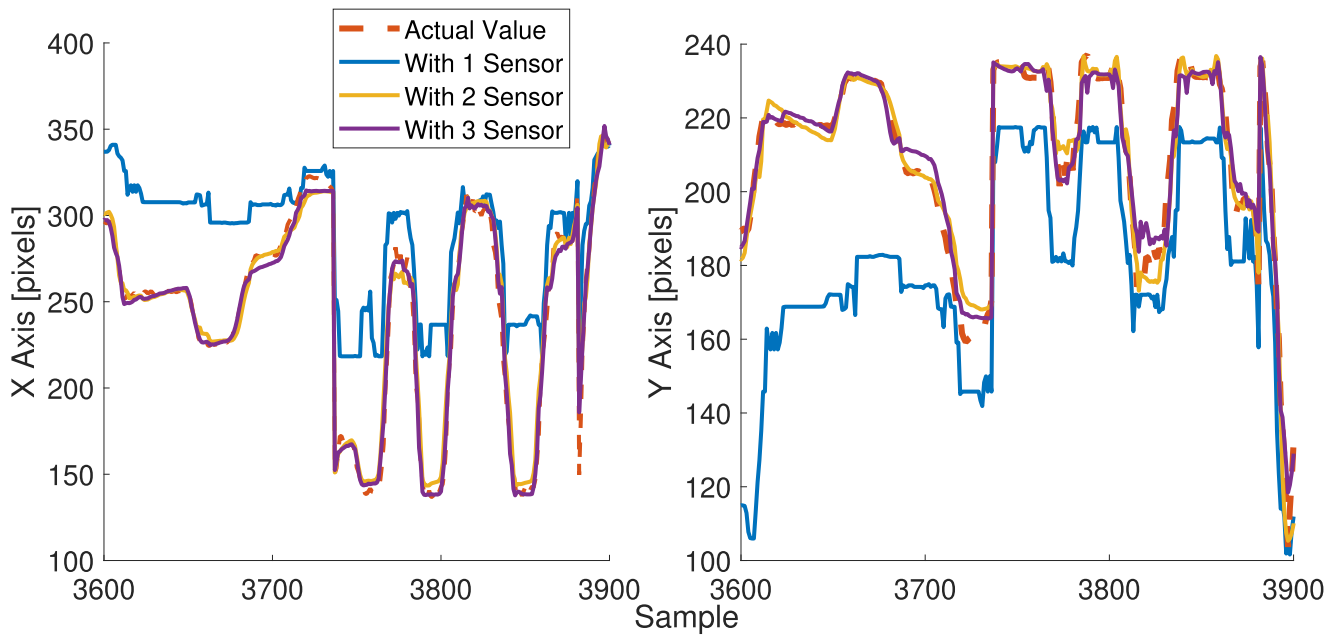


Fig. 13. Estimating the pixel coordinates of the end-effector of the soft actuator with different combinations of the soft strain sensors (The best combination is selected for each). Almost all the effects of drift and hysteresis can be compensated with the addition of redundant variable soft sensors.

the same matrix as the actuator, some of the sensors are coated with a thin layer of different material before being placed in the actuator. In order to maintain compatibility with the actuator material (Ecoflex), we use only three type of embedding matrix for the sensors; DragonSkin, Natural Rubber and Ecoflex itself. As the coating on the strain is thin, the introduction of the new material does not affect the physical properties of the sensor much. Pseudorandom actuation patterns are input to the finger and the corresponding sensor resistances and finger tip positions are recorded. 15 000 data points are collected using a 12-bit resolution DAQ.

The prediction accuracy for each individual sensor along with their mutual information with the bending angle is shown in Fig. 11. Just like the linear strain case, the mutual information metric is still a good indicator of the sensor performance. Note that there is some variability in the performance of the sensors even if they are embedded in same matrix. This can be expected as now there is an additional interface introduced by the actuator material, which can further affect the stress distribution around the sensor. Similar analysis for all the two sensor combinations are shown in Fig. 12. The figure is plotted based on the sorted MI values to show the correlation between MI and the prediction error. Note that prediction accuracy obtained through the learning process is not necessarily a good measure of the sensor quality, as they are prone to overfitting the data.

The improvement in prediction accuracy with the increase in redundant sensor configuration is shown in Fig. 14. It can be seen that significant improvements in prediction accuracy can be obtained by additional strain sensors. The real predicted values of the marker using the learned model and the best combination of sensors are shown in Fig. 13 for reference. Even with two sensors, it is clear that an accurate estimation of strain can be

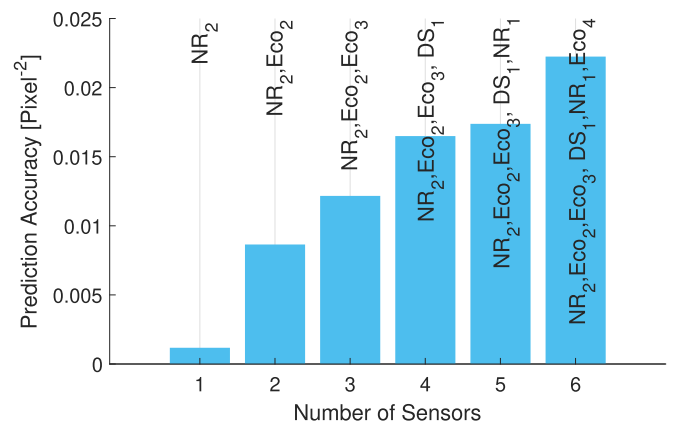


Fig. 14. Improvement in static strain sensing accuracy with the addition of redundant and disjoint soft strain sensors for the bending actuator. The prediction accuracy for the best combination is shown here.

obtained without taking into account the past history of the sensor.

## V. CONCLUSION

This letter presents a methodology for using redundant and disjoint soft robotic sensors for accurate static strain estimation. The main idea behind this letter is to compensate for the time-variant hidden states of a soft-bodied system using these redundant and disjoint sensors to finally obtain the true strain state in a static manner. Theoretical underpinnings of the concept is demonstrated through information theoretics and learning-based methods are used to validate the theory. Our results are a demonstration that quantity can upend quality,

especially for soft strain sensors where variability is intrinsic to most manufacturing processes and high quality sensors are very difficult to develop and fabricate. As the state estimation is done using only current sensor data, the processing and learning architecture is greatly simplified when compared to modelling with recurrent neural networks. We also introduce Mutual Information as a quick measure of the quality of the sensors. It can also be used to compare different sensors in a universal manner. In the paper we train all the combinations of sensors to compare their performances. This is not required in actual applications. We can use the MI measures to pick the best combinations or use all the available sensors, which will guarantee the best performance.

The true potential of our methodology can be realized with fabrication and data processing techniques that can create and process a large number of soft sensors. As the algorithm favours variability among sensors, intrinsic variabilities in the manufacturing process is advantageous. Higher variabilities can be introduced with multi-material fabrication, as we show in this letter. This approach can also be used to design optimized sensory structures [17], [26], [27]. Future works include scaling up the experimental setup for high-dimensional state estimation and for closed-loop control with feedback from embedded sensors.

#### REFERENCES

- [1] M. Amjadi, K.-U. Kyung, I. Park, and M. Sitti, "Stretchable, skin-mountable, and wearable strain sensors and their potential applications: A review," *Adv. Funct. Mater.*, vol. 26, no. 11, pp. 1678–1698, 2016.
- [2] H. Wang, M. Totaro, and L. Beccai, "Toward perceptive soft robots: Progress and challenges," *Adv. Sci.*, vol. 5, no. 9, 2018, Art. no. 1800541.
- [3] R. K. Kramer, C. Majidi, R. Sahai, and R. J. Wood, "Soft curvature sensors for joint angle proprioception," in *IEEE/RSJ Int. Conf. Intell. Robots Syst.*, 2011, pp. 1919–1926.
- [4] Y.-L. Park, C. Majidi, R. Kramer, P. Bérard, and R. J. Wood, "Hyperelastic pressure sensing with a liquid-embedded elastomer," *J. Micromechanics Microengineering*, vol. 20, no. 12, 2010, Art. no. 125029.
- [5] S. Russo, T. Ranzani, H. Liu, S. Nefti-Meziani, K. Althoefer, and A. Menciassi, "Soft and stretchable sensor using biocompatible electrodes and liquid for medical applications," *Soft Robot.*, vol. 2, no. 4, pp. 146–154, 2015.
- [6] C. Mattmann, F. Clemens, and G. Tröster, "Sensor for measuring strain in textile," *Sensors*, vol. 8, no. 6, pp. 3719–3732, 2008.
- [7] N. Hu *et al.*, "Investigation on sensitivity of a polymer/carbon nanotube composite strain sensor," *Carbon*, vol. 48, no. 3, pp. 680–687, 2010.
- [8] A. Georgopoulou and F. Clemens, "Piezoresistive elastomer-based composite strain sensors and their applications," *ACS Appl. Electron. Mater.*, vol. 2, no. 7, pp. 1826–1842, 2020.
- [9] S. Sareh *et al.*, "Bio-inspired tactile sensor sleeve for surgical soft manipulators," in *Proc. IEEE Int. Conf. Robot. Automat.*, 2014, pp. 1454–1459.
- [10] H. Liao, X. Guo, P. Wan, and G. Yu, "Conductive mxene nanocomposite organohydrogel for flexible, healable, low-temperature tolerant strain sensors," *Adv. Funct. Mater.*, vol. 29, no. 39, 2019, Art. no. 1904507.
- [11] G. Cai, J. Wang, K. Qian, J. Chen, S. Li, and P. S. Lee, "Extremely stretchable strain sensors based on conductive self-healing dynamic crosslinks hydrogels for human-motion detection," *Adv. Sci.*, vol. 4, no. 2, 2017, Art. no. 1600190.
- [12] J. T. Muth *et al.*, "Embedded 3D printing of strain sensors within highly stretchable elastomers," *Adv. Mater.*, vol. 26, no. 36, pp. 6307–6312, 2014.
- [13] N. Hu and H. Fukunaga, "Piezoresistive strain sensors made from carbon nanotubes-based polymer nanocomposites," *Sensors*, vol. 11, no. 11, pp. 10 691–10 723, 2011.
- [14] A. Georgopoulou, C. Kummerlöwe, and F. Clemens, "Effect of the elastomer matrix on thermoplastic elastomer-based strain sensor fiber composites," *Sensors*, vol. 20, no. 8, 2020, Art. no. 2399.
- [15] B. Shih *et al.*, "Electronic skins and machine learning for intelligent soft robots," *Sci. Robot.*, vol. 5, no. 41, 2020.
- [16] K. Chin, T. Hellebrekers, and C. Majidi, "Machine learning for soft robotic sensing and control," *Adv. Intell. Syst.*, vol. 2, no. 6, 2020, Art. no. 1900171.
- [17] T. G. Thuruthel, J. Hughes, and F. Iida, "Joint entropy-based morphology optimization of soft strain sensor networks for functional robustness," *IEEE Sensors J.*, vol. 20, no. 18, pp. 10801–10810, Sep. 2020.
- [18] T. G. Thuruthel, B. Shih, C. Laschi, and M. T. Tolley, "Soft robot perception using embedded soft sensors and recurrent neural networks," *Sci. Robot.*, vol. 4, no. 26, 2019.
- [19] S. Han, T. Kim, D. Kim, Y.-L. Park, and S. Jo, "Use of deep learning for characterization of microfluidic soft sensors," *IEEE Robot. and Automat. Lett.*, vol. 3, no. 2, pp. 873–880, Apr. 2018.
- [20] T. G. Thuruthel, K. Gilday, and F. Iida, "Drift-free latent space representation for soft strain sensors," in *Proc. 3rd IEEE Int. Conf. Soft Robot.*, 2020, pp. 138–143.
- [21] D. Kim, J. Kwon, B. Jeon, and Y.-L. Park, "Adaptive calibration of soft sensors using optimal transportation transfer learning for mass production and long-term usage," *Adv. Intell. Syst.*, vol. 2, no. 6, 2020, Art. no. 1900178.
- [22] R. Pascanu, T. Mikolov, and Y. Bengio, "On the difficulty of training recurrent neural networks," in *Proc. Int. Conf. Mach. Learn.*, 2013, pp. 1310–1318.
- [23] M. Park, Y. Ohm, D. Kim, and Y.-L. Park, "Multi-material soft strain sensors with high gauge factors for proprioceptive sensing of soft bending actuators," in *Proc. 2nd IEEE Int. Conf. Soft Robot.*, 2019, pp. 384–390.
- [24] A. Kraskov, H. Stögbauer, and P. Grassberger, "Estimating mutual information," *Phys. Rev. E*, vol. 69, no. 6, 2004, Art. no. 0 66138.
- [25] G. Brown, A. Pocock, M.-J. Zhao, and M. Luján, "Conditional likelihood maximisation: A unifying framework for information theoretic feature selection," *J. Mach. Learn. Res.*, vol. 13, no. 1, pp. 27–66, 2012.
- [26] V. Wall and O. Brock, "Multi-task sensorization of soft actuators using prior knowledge," in *Proc. Int. Conf. Robot. Automat.*, 2019, pp. 9416–9421.
- [27] J. Tapia, E. Knoop, M. Mutny, M. A. Otaduy, and M. Bächer, "Makesense: Automated sensor design for proprioceptive soft robots," *Soft Robot.*, vol. 7, no. 3, pp. 332–345, 2020.